Biomed Microdevices (2007) 9:801–808
DOI 10.1007/s10544-007-9092-0

Magnetic microparticle steering within the constraints of an MRI system: proof of concept of a novel targeting approach

Jean-Baptiste Mathieu · Sylvain Martel

Published online: 14 June 2007

Abstract This paper presents a magnetic microparticle steering approach that relies on improved gradient coils for Magnetic Resonance Imaging (MRI) systems. A literature review exposes the motivation and advantages of this approach and leads to a description of the requirements for a set of dedicated steering gradient coils in comparison to standard imaging coils. An experimental set-up was developed to validate the mathematical models and the hypotheses arising from this targeting modality. Magnetite Fe_3O_4 microparticles (dia. 10.9 μm) were steered in a *Y*-shaped 100 μm diameter microchannel between a Maxwell pair (dB/dz= 443 mT/m) located in the center of an MRI bore with 0.525 m/s mean fluid velocity (ten times faster than in arterioles with same diameter). Experimental results based on the percentage of particles retrieved at the targeted outlet show that the mathematical models developed provide an order of magnitude estimate of the magnetic gradient strengths required. Furthermore, these results establish a proof of concept of microparticle steering using magnetic gradients within an MRI bore for applications in the human cardiovascular system.

This project is supported in part by a Canada Research Chair (CRC) in Micro/Nanosystem Development, Fabrication and Validation, the Canada Foundation for Innovation (CFI), the National Sciences and Engineering Research Council of Canada (NSERC), Fonds Québécois de la Recherche sur la Nature et les Technologies (FQRNT), Fonds de la Recherche en Santé du Québec (FRSQ) and the Government of Québec.

J.-B. Mathieu · S. Martel (✉)
Department of Computer Engineering and the Institute of Biomedical Engineering, NanoRobotics Laboratory, École Polytechnique de Montréal (EPM), Montréal, Québec, Canada
e-mail: sylvain.martel@polymtl.ca

J.-B. Mathieu
e-mail: jean-baptiste.mathieu@polymtl.ca

Keywords Magnetic microparticle steering · Gradient coils · Maxwell pair · MRI systems

1 Introduction

Medical applications of magnetic guidance have been studied for more than fifty years (Frei 1972). Removal of foreign metallic bodies using external magnets was one of the first applications envisioned. Then the concept evolved and applications like steering of magnetic tipped catheter (Alksne 1968) and endovascular treatment of intracranial aneurism using Iron particles (Alksne 1970) emerged. Nowadays, the catheter steering approach is commercially available from Stereotaxis (2006) while the aneurism treatment approach is mostly discarded in favour of Guglielmi's coils (Guglielmi et al. 1991a,b). In the 1980s, the Video Tumor Fighter (VTF) project aimed at controlling a small magnet through brain tissue. This small magnet was brought inside a tumour using an external electromagnet and was heated using Radio Frequency (RF) in order to deliver hyperthermia (Grady et al. 1989, 1990a,b; Howard et al. 1989; Molloy et al. 1990). The VTF and Niobe systems by Stereotaxis have common roots and both rely on X-ray fluoroscopy projections for tracking.

Applications using magnetic particles as drug delivery carriers have been described as early as the end of the seventies (Mosbach and Schroder 1979; Senyei et al. 1978). Ever since, most of the research effort seems to have been placed on particles and carriers development (Alexiou et al. 2001, 2002; Babincova et al. 1999, 2001, 2002, 2004; Lemke et al. 2004; Morales et al. 2005; Nobuto et al. 2004; Viroonchatapan et al. 1995) while the targeting and tracking methods remained almost unchanged.

The most common targeting strategy relies on injecting the particles intravenously and on placing the strongest possible magnet next to the tissue to be targeted. Trapping is ensured by friction of the particles on the vessel wall (Mykhaylyk et al. 2005). For the remainder of the text, this approach will be referred to as "Classical Magnetic Targeting" (CMT). Its main drawback is that it is limited to organ close to the surface of the skin or to murine specimens. This limitation was mathematically demonstrated in (Grief and Richardson 2005) where they state that it is impossible to target regions deep within the body using an external magnet without targeting some surrounding regions more strongly. Some improvements over classical magnetic targeting rely on magnet tipped catheters (Alksne 1968), magnetic needles, wires or stents (Iacob et al. 2004; Forbes et al. 2003; Yellen et al. 2003, 2005) to reach internal organs. Nevertheless, the non linear geometry of the induced field and the resulting distribution of the particles remain uncontrolled.

The magnetic force F (N) acting on a magnetized body is proportional to its magnetic moment m (A.m^2) and to the gradient of the magnetic field H (A/m) as shown in Eq. 1 where μ_0 (N.A^{-2}) is the permeability of vacuum.

$$\vec{F}_{\text{mag}} = \mu_0.(\vec{m}.\nabla)\vec{H} \tag{1}$$

In this paper, we show that the characteristics of modern Magnetic Resonance Imaging (MRI) systems can be used to address the magnetic limitations of the CMT approach. By providing linear spatial encoding magnetic gradients, they can be used to induce a force on a magnetized body. This force is constant wherever the magnetized body is located inside the field of view of the MRI (Martel et al. 2004; Mathieu et al. 2005, 2006).

MRI systems offer a level of control and flexibility over particles distribution that cannot be achieved by classical magnetic targeting.

Besides addressing the purely magnetic limitations of the classical approach, MRI systems also provide concentration and tracking information, real-time interventional capabilities and are already widespread in hospitals.

A medium term research strategy would be to produce biodegradable microparticles with tunable degradation time and a diameter slightly larger than the lumen of human capillaries as first generation devices. Particle sizes in the order of 5–20 μm diameters are envisioned. Once guided using an MRI based navigation platform to a predefined target area, these particles will embolize in the capillaries and dissolve while releasing an active principle. This approach does not require extra propulsion power to sustain blood flow once particles have reached targeted tissues and ensures confined drug release. The composition and molecular weight of the polymer chains allow tuning of the pharmacokinetics as well as of microcarrier degradation time required to unblock the capillary network. A longer term approach could comprise an active and reversible anchoring mechanism (either mechanical or chemical) that could be embedded in future micro/nanodevices.

In this paper, we propose an experimental MRI steering set-up designed to approach the conditions of our first generation devices. Hence Fe_3O_4 magnetic particles with average size (10.9±1.6 μm) slightly larger than the lumen of human capillaries were chosen. These particles were steered using a custom Maxwell pair (443 mT/m gradient) inside of a 100 μm microvascular channel (0.5 m/s average fluid velocity) placed at the center of the bore of a clinical MRI system.

2 Dedicated steering coils

Clinical MRI gradient coils are designed with imaging constraints in mind and generate typical maximum amplitudes of approximately 40 mT/m. Such gradient amplitude, while sufficient to propel millimetric magnetized spheres (Mathieu et al. 2005, 2006), appears to be more than two orders of magnitude lower than what is required for nanoparticles targeting (Mykhaylyk et al. 2005). Table 1 presents classical magnetic targeting strategies.

As a solution, additional steering gradient coils with higher gradient strengths are proposed to be installed in the MRI bore and to operate synchronously in a time-multiplexed fashion with the MR-imaging coils.

In (Mykhaylyk et al. 2005) several T/m gradients are used for efficient steering of Magnetite nanoparticles in mice blood vessels. Figure 1 shows predictions of microparticle steering gradients range. In addition to predicting the gradients required for microparticles in 5 and 10 μm human capillaries, a third curve was plotted in accordance to the conditions of our experimental set-up. Bold vertical bars show the magnetic gradient required to bring a magnetic particle past the centerline of a given microchannel before the next symmetric bifurcation. This simple criterion served as an experimental set-up design rule of thumb. It was used to set the gradient amplitude and flow velocity inside the microvascular channel proposed in this paper.

Gradients in the 100–500 mT/m range are required for steering microparticles in these microchannels. This only represents one order of magnitude increase compared to standard MRI gradient amplitude. Such upgrade seems achievable when human sized gradient coil design constraints are taken into account.

Measures of coil performance are dependant upon specific requirements related to the application (Turner 1993). These measures include coil efficiency η (gradient per unit current), inductance L, power dissipation W and gradient homogeneity.

Table 1 Examples of recent trapping strategies

Method	Ref
Magnetoliposomes: magnetite 10 nm, Electromagnet: field strength between two poles>0.3 T (0.4 T max) when poles are 1 cm apart applied for 15, 30, 45, 60, 100 min.	(Nobuto et al. 2004)
100 nm (hydrodynamic diameter) starch covered magnetic particles 10 min application of ferrofluid, 50 min external magnetic field (e.g. at a distance of 10 mm to the tip of the pole shoe the flux density was B=1.0 T, the gradient was dB/dx=30 T/m)	(Alexiou et al. 2001)
Ne–Fe–B magnets were arranged above the target area with a frame attached to the patient's bed and in minimal distance (less than 0.5 cm) to the tumor. Up to ten magnets (8×4×2 cm or 3×3×1 cm) resulted in a total field of at least 0.5 T and in general 0.8 T.	(Lemke et al. 2004)
Dextran magnetite (DM) particles 5–10 nm (average 8 nm) incorporated inside thermosensitive magnetoliposomes (1.16+−0.37 μm) Coercivity=240 A/m, magnetic susceptibility 0.3 $(gFe)^{-1}$, saturation magnetization=0.1 Wb/m^2.gFe and T2 relaxivity=220 $l.mmol^{-1}.s^{-1}$.	(Viroonchatapan et al. 1995)

There are three phases in gradient pulses: Rise Time (RiT), Up Time (UT) and Fall Time (FT) (Fig. 2).

MRI gradient coils are designed to provide rise time as short as 200 μs due to proton relaxation times. Hence, low inductance appears to be a dominant design parameter for imaging. While gradient amplitude can be limited by low inductance requirements, coil resistance has to be minimized due to cooling system design issues. They can be powered approximately 50% of the time when supplied with maximum allowed current.

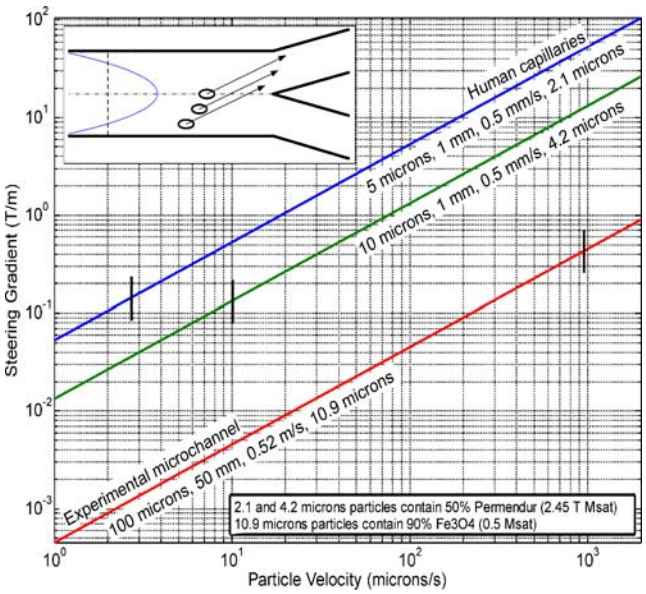

Fig. 1 Steering gradient versus particle velocity. *Bold vertical bars* show the magnetic gradient required to bring a magnetic particle past the centerline of a given microchannel before the next symmetric bifurcation. Channel and particle simulation parameters are displayed underneath curves with format: "channel diameter, channel length, average velocity of Poiseuille flow, particle diameter." Steering gradients for 2.1 and 4.2 μm diameter containing 50% volume Permendur sphere in human capillaries with diameters of 5 and 10 μm (physiological specifications from (Charm and Kurland 1974; Whitmore 1968). Steering gradients for 10.9 μm Fe_3O_4 particles were simulated accordingly to conditions described in Section 3. One hundred to five hundred milliteslas per meter gradients are required for steering of 2.1, 4.2 and 10.9 μm particles in such vessels

Envisioning steering gradient coils for magnetic microparticles requires dealing with those same design constraints but with a different priority order. Rise time is a secondary parameter for steering coils. The first reason is that unlike imaging gradients, steering gradients can be effective even in transient state. The second reason is that the gradient switching frequency of the interleaved propulsion phases in our control loops (Chanu et al. 2006) is lower than 100 Hz while it can be ten times higher during fast MRI sequences. Steering gradient pulses need to be as long as sustainable by gradient coils/amplifiers in order to maximize the effect of steering force. Hence, a rise time of a few milliseconds seems acceptable in the context of steering coils.

Since gradients with maximum amplitudes must be generated for steering, gradient efficiency is the parameter to optimize. In this context, power dissipation becomes the limiting factor. The gradient amplitude varies linearly with the number of winding N and current I, while power dissipation W varies linearly with N and I^2. Therefore, since $\nabla B \propto NI$, $W \propto NI^2$ increasing winding number N at the expense of inductance L to reduce the current I is a practical approach to loosen the power dissipation limitations and allows an increase of the duty cycle. If steering

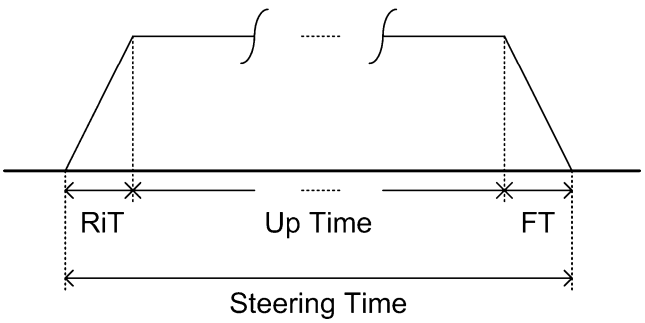

Fig. 2 Description of a Gradient pulse

gradient coils are to be built, their gradient strength should have priority over their inductance and linearity. Increased inductance will lead to a longer rise time and fall time that will prevent them from being used for imaging. Therefore, standard imaging coils would still be used for tracking purposes. The two sets of coils would be powered in a time multiplexed fashion in order to alternate propulsion and tracking phases as fast as possible.

The theoretical gradient amplitude steering coils should generate in order to improve targeting efficacy of microparticles needs to be validated experimentally. A small scale Maxwell pair able to generate a one-dimensional gradient along the longitudinal axis of an MRI system is used to steer microparticles inside a micro-channel. This set-up aims at gathering experimental data in order to validate our predictions of the steering gradient amplitude range for microparticle in an MRI system. For that purpose, a Maxwell pair is a simple and effective solution even though it only allows one dimensional steering. Once experimental validation is performed, the gradient amplitude range becomes a design requirement for a 3D insert. Such insert will be able to generate a steering force in any direction of space by vectorial sum of the gradient generated by each coil. Hence, control in any possible direction for blood vessel bifurcation can be performed. It will be used to generate extensive data in 1D, 2D and 3D microvascular channels.

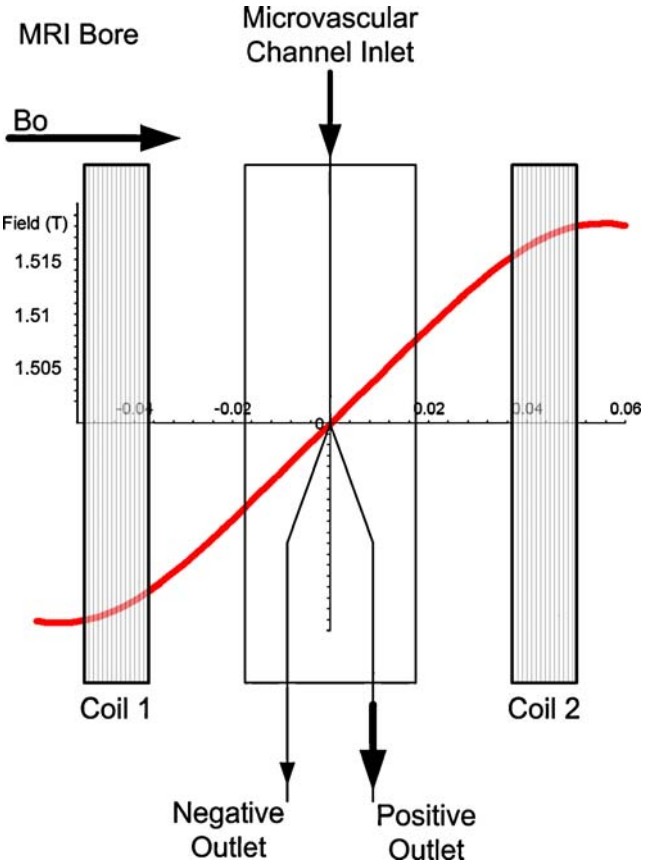

Fig. 3 Schematic of the magnetic suspension steering set-up. Coils 1 and 2 belong to Maxwell pair

3 Materials and methods

Modelization of the interactions taking place while steering a magnetic microparticle suspension in presence of blood constituents inside a tumour angiogenic circulation is of formidable complexity. One has to associate a model or scan of tumour angiogenic network (Abdul-Karim et al. 2003; McDougall et al. 2002; Varghese et al. 2005) with ferrohydrodynamics and colloid interparticle interactions which include London–Van Der Waals potential, electrostatic double layer, electrosteric repulsion, magnetic dipole (Rosensweig 1997), Stokes law of fluid friction weighted by a wall effect correlation (Fidleris and Whitmore 1961; Kehlenbeck and Di Felice 1999) and to a lower extent gravity and Brownian motion.

As a first validation step, a simple *Y*-shaped microvascular channel geometry was chosen for better experimental parameters control and data analysis simplicity.

In this set-up, the B_0 static field of the MRI system is used to magnetize the microparticles up to their saturation; the gradient from the Maxwell pair is used to induce a constant magnetic force on the entire microvascular channel and to choose a preferential outlet or branch of the *Y*-shaped channel, as shown in Fig. 3.

3.1 Maxwell pair

The longitudinal component of the magnetic field and the magnetic field gradient produced by two electrical current loops are given by Eqs. 2 and 3, respectively.

$$B(z) = N^*\left(\frac{\mu_0 i a^2}{2\left(\left(\frac{1}{2}d - z\right)^2 + a^2\right)^{3/2}} - \frac{\mu_0 i a^2}{2\left(\left(\frac{1}{2}d + z\right)^2 + a^2\right)^{3/2}}\right) + B_0 \tag{2}$$

$$\frac{dB(z)}{dz} = N^*\left(-\frac{3\mu_0 i a^2(-d+2z)}{4\left(\left(\frac{1}{2}d - z\right)^2 + a^2\right)^{5/2}} + \frac{3\mu_0 i a^2(d+2z)}{4\left(\left(\frac{1}{2}d + z\right)^2 + a^2\right)^{5/2}}\right) \tag{3}$$

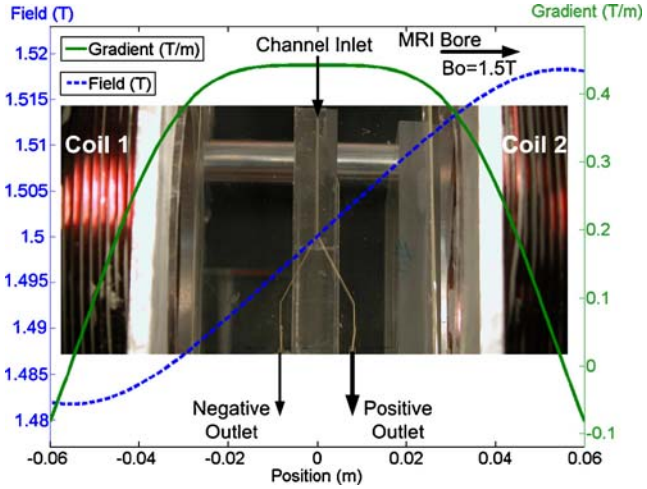

Fig. 4 Magnetic field and gradient of the Maxwell pair (I=20A)

In the above equations, N=100 is the number of windings in the coil, a the radius of the current loop, μ_0 the vacuum permeability, i the electrical current, d the distance between the coils, z the position along the longitudinal axis of the loops and B_0 the static field of the MRI system.

Equation 4 shows a Taylor/McLaurin power series expansion of dB/dz keeping only the first order term.

$$\frac{dB}{dz} \approx 48^{*}N^{*}\frac{\mu_0 i a^2 d}{(d^2+4a^2)^{5/2}} + O(z) \tag{4}$$

A Maxwell pair is a simple two coil arrangement used to generate a linear magnetic field gradient. The coils are separated by a distance $a \times 3^{1/2}$ and supplied with equal but opposed currents. This configuration minimizes all but the linear longitudinal term of the field (Fig. 4). Table 2 lists the main specifications of our Maxwell pair. A TTi TSX 1820P DC power supply was used for the purpose of the experiment (Thurlby Thandar Instruments 2006).

3.2 Iron oxide suspension

A magnetic suspension from Bangs Laboratories (Bangslabs 2006) containing Iron Oxide magnetic particles in distilled water with an average particle size of 10.9±1.6 μm) was used. Saturation magnetisation of the magnetic suspension was measured M_{sat}=92 emu/g. Magnetic particles in the suspension contain above 90% magnetite weight fraction. Hence, a minimum particle saturation magnetisation of 82.8 emu/g is expected. Equilibrium of forces between magnetic force and Stokes law of fluid friction weighted by a wall effect correlation (Kehlenbeck and Di Felice 1999) allows for a theoretical particle terminal velocity calculation (Fidleris and Whitmore 1961). A 443 mT/m gradient applied on 10.9 μm particles with magnetic moment m= 82.8 emu/g inside a 100 μm cylindrical channel yields a theoretical magnetophoretic terminal velocity is 956 μm/s.

Table 2 Specifications of the Maxwell pair

Specification	Description
Wire	Cu wire, AWG 13, square section, high temperature insulation, supplied by MWS wire industries http://www.mwswire.com/
Maximum current	20 A
Maximum gradient (20 A)	0.443 T/m
Winding	100 turns
Radius	0.0603 m

3.3 Microvascular channel

A *Y* shaped 100 μm diameter microvascular channel (Fig. 5) with a 5 cm long inlet channel splitting towards two 100 μm diameter outlet channels was fabricated by direct-write assembly (Therriault et al. 2003).

The microvascular channel's split is placed at the center point of both a Maxwell pair and the MRI bore. The magnetic particles suspension is injected through the inlet of the microvascular channel. While travelling through the channel longitudinally because of the flow, the magnetic particles cross the radius of the channel transversally because of the magnetic force. A difference in the quantity of suspension being collected at each of the two outlets is caused by the magnetic gradient generated by the Maxwell pair. For convenience, the channel towards which the particles are deflected is defined here as the positive outlet.

This experiment aims at comparing the percentage of the Iron Oxide particles driven towards the positive outlet channel when the Maxwell pair is *on* versus when it is *off*. A larger targeting efficacy (yield) is correlated with a larger percentage of the particles reaching the positive outlet.

Yield is defined as the ratio of the number of particles in the positive outlet of the channel over the total number of particles.

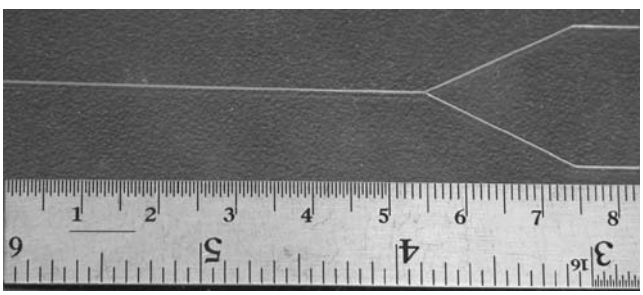

Fig. 5 *Y*-shaped microvascular channel fabricated by direct write assembly

3.4 Experimental protocol

The maximum flow Q_{max} is calculated from the theoretical 956 μm/s magnetophoretic terminal velocity of the particles. According to the steering rule of thumb described sooner, all the particles located on the same side of the centerline of the channel prior to the *Y* split should exit through the same outlet. Hence, according to this set-up design criterion, if all the particles travel half the channel's diameter (50 μm), one should expect a 100% steering efficiency. The time required for the particles to cross 50 μm while travelling at 956 μm/s is t=0.0523 s.

Therefore, the longitudinal flow velocity is calculated in order to allow the particle a t=2×0.0523 s=0.104 s transit time in the channel prior to the split. A "factor of safety" of 2 is arbitrarily applied to compensate for the simplicity of both the steering criterion and the terminal velocity calculation method. This transit time yields an average fluid velocity v_{av}=0.5 m/s inside the channel.

A parabolic flow velocity profile in the channel is expected. Such flow profile yields an average velocity v_{av}= 0.5 m/s inside the channel. The theoretical maximum velocity being v_{max}=2 * v_{av}=1.05 m/s at the centerline of the channel (White 1999).

The flow was set to Q=v_{av} * A=0.25 ml/min using a New Era NE-1000 programmable syringe pump (New Era Pump systems 2006) located outside the bore of the MRI system. A is the cross sectional area of the channel. The quantity of particles at each outlet of the microvascular channel was measured by optical density using a Varian Cary 50 Bio UV Visible spectrophotometer (Varian 2006). Tests were conducted as shown in Table 3.

This protocol was repeated two times for each gradient polarity (+443 and −443 mT/m), N=4 for the positive outlets. All experiments were performed on a clinical scanner (Siemens Magnetom Vision 1.5 T, Erlangen, Germany). For each data point, at least 1 ml of magnetic suspension was injected in the microvascular channel during 4 min while maintaining an average fluid velocity of 0.5 m/s. The gradient coil insert was designed to generate a high gradient. Since it is air cooled and temperature in the core of the windings reaches 80°C after 10 min with 20 A (443 mT/m), 30–40 min was required after every single injection to allow the system to cool down to 27°C. Considering this cooling period with the time required for sample preparation results to approximately 1 h per data point. More than 7 h on an MRI scanner was required to gather the experimental data.

3.5 Simulations of yield

A microvascular channel with same length and diameter than the experimental one was simulated using MatLab. Magnetic particles were generated with random origins for every particle. Their trajectories were computed while subjected to a magnetic gradient and to parabolic flow profiles. Several simulations of yield versus particle diameters and flow were averaged and plotted.

Some assumptions were made to simplify the model. First, it was assumed that the outlet a particle would be steered into is determined according to its position with respect to the centerline of the channel only. Second assumption was to neglect interactions between the particles and the walls of the channel. Third assumption was to neglect magnetic particle-to-particle interactions. Even though this last assumption is common in recent literature (Aviles et al. 2005; Kim et al. 2006), its impact regarding particle aggregate shape and size is believed to affect yield significantly. Nevertheless, the mathematical complexity of particle-to-particle interactions requires models that are beyond the scope of this paper.

4 Results and discussion

As shown in Fig. 6, a Maxwell pair providing a 443 mT/m gradient was used to steer magnetite microparticles inside a microvascular channel. An increased amount of particles was measured at the positive outlet (left hand outlet when the gradient pointed leftward and right hand outlet when the gradient pointed rightward).

The proposed steering method relying on the deflection of magnetic particles while travelling along the flow towards a preferential direction is validated. Nevertheless, a higher than 60% targeting efficacy would be suitable in the positive outlet within the constraints imposed by clinical MRI systems. While a 85% fraction was achieved in (Pekas et al. 2005), their experimental conditions differ

Table 3 Experimental protocol

Pre control *Off*	Gradient applied *On*	Post control *Off*
1.5 ml of suspension Injected. Gradient is Off	1.5 ml of suspension Injected. Gradient is applied towards the left or right hand side of the inlet channel.	1.5 ml of suspension injected. Gradient is Off
0.75 ml is collected at each outlet.	0.75 ml is collected at each outlet.	0.75 ml is collected at each outlet.

too much from ours to allow any direct comparison. In our study, the diameter of the microvascular channel was chosen to emulate a human arteriole. Its length was maximized within the radius of the coils in order to increase steering efficacy. Nevertheless, the fluid velocity inside the channel is much higher than stated in physiological data charts and is closer to arterial flow. These choices were made in order to reduce the duration of each individual trial during the experiments and to increase the number of samples *N*.

According to the simulations of yield, a 100% efficiency was to be expected. This steering criterion and the theoretical model used are simplified and it must be remembered that they are merely experimental set-up design rules of thumb. Critical parameters such as interactions with channel walls, particle magnetic aggregation, and dependence of aggregate size on terminal velocity and yield were not taken into account.

It is to note that when aggregate size becomes similar to the diameter of the channel, the assumptions underlying the calculations of yield can not be relied on anymore. As a matter of fact, it was observed that aggregates made of magnetic particles form and dissolve to fit in the channel. Therefore, a large aggregate reaching the *Y* branch might split regardless of the position of its center of mass with respect to the centerline of the channel. A strong correlation between aggregate size and suspension concentration is expected and further studies will focus on this topic.

Nevertheless, gradient amplitude range predictions are in the right order of magnitude and, to our point of view, confirm the viability of the proposed steering method.

A tentative extrapolation of the impact of particle size and flow on yield is proposed (Fig. 7). Theoretical curves were fitted on experimental data. A correction factor of 0.4 was applied to the magnetophoretic velocity of the particles. This factor was chosen because it allows a fit between the 0.5 m/s average flow curve with 10.9 μm particles and the experimental data (box on Fig. 7). From Fig. 7, yield is predicted to increase with lower flows and larger particle sizes or aggregates.

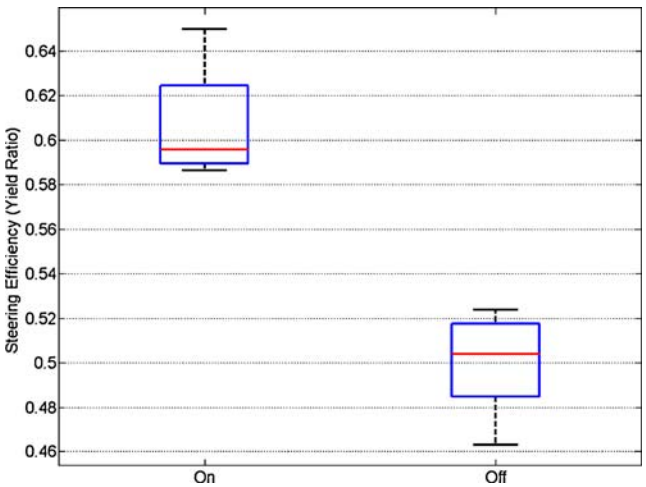

Fig. 6 Box plot showing experimental measurement of yield. The 'On' *box* shows the yield when the gradient coil is supplied with 20 A current (average=0.61), the 'Off' *box* shows the yield when the gradient coil is turned off (average=0.5). *Box* plots show no overlap between the yield distributions

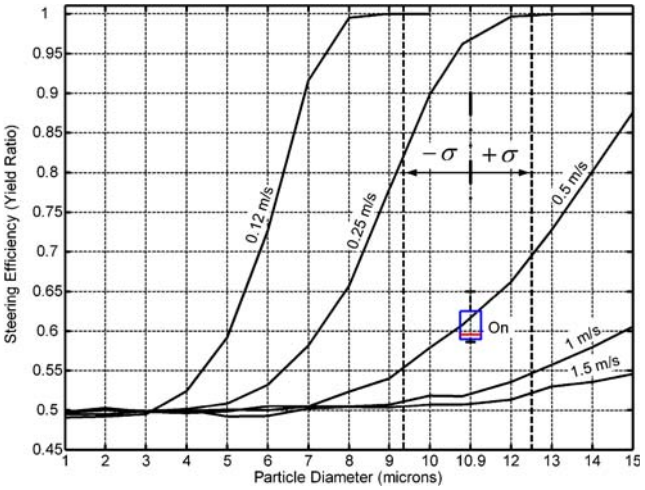

Fig. 7 Simulated impact of flow and particle size on average yield of Fe_3O_4 particles in water. Channel diameter and length are 100 μm and 50 mm respectively; magnetic gradient is 443 mT/m. A Poiseuille flow profile was simulated. Average velocity of the flow profile is displayed above each curve. Experimental data box from Fig. 6 was superimposed on simulated data. *Dashed vertical lines* indicate average and standard deviation values from the size distribution of the magnetic suspension used in experimental set-up

This manuscript aims at providing a preliminary proof of the feasibility of steering magnetic microparticles using modified gradient coils inside an MRI system. Similar tests with different flow rates, suspension concentrations, channel diameters and gradient amplitudes will be performed to further refine our models. Once a fit is achieved between theoretical and experimental data and required gradient amplitudes and scaling laws well characterized, a multilayer steering gradient coil insert for animals will be designed and built using a target field method (Chronik et al. 1999; Turner 1986, 1988).

It will be used to implement 3D control loops for magnetic suspension relying on imaging gradient coils for tracking and on steering gradient coils for targeting. The long term motivation is magnetic microparticles controlled delivery in tumour angiogenic networks for chemoembolization applications.

Acknowledgments The authors wish to thank Pr. Daniel Therriault and Jean-François Dufresne for their support in the design and fabrication of the microvascular networks, Pr. David Ménard and Louis-Philippe Carignan for VSM measurements and Mahmood Mohammadi for his support with the light absorption measurements.

Reference

M.A. Abdul-Karim, K. Al-Kofahi, E.B. Brown, R.K. Jain, B. Roysam, Microvasc. Res. **66**, 113–125 (2003)

C. Alexiou, W. Arnold, P. Hulin, R.J. Klein, H. Renz, F.G. Parak, C. Bergemann, A.S. Lubbe, J. Magn. Magn. Mater. **225**(1–2), 187–193 (2001)

Ch. Alexiou, A. Schmidt, R. Klein, P. Hulin, Ch. Bergemann, W. Arnold, J. Magn. Magn. Mater. **252**(1–3 Spec Iss), 363–366 (2002)

J.F. Alksne, Surgery **64**, 339–45, (1968).

J.F. Alksne, Neurology **20**, 376 (1970)

M.O. Aviles, A.D. Ebner, H. Chen, A.J. Rosengart, M.D. Kaminski, J.A. Ritter, J. Magn. Magn. Mater. **293**(1), 605–615 (2005)

M. Babincova, P. Sourivong, D. Chorvat, P. Babinec, J. Magn. Magn. Mater. **194**(1–3), 163–166 (1999), Proceedings of 1998 2nd International Conference on Scientific and Clinical Applications of Magnetic Carriers.

M. Babincova, D. Leszczynska, P. Sourivong, P. Cicmanec, P. Babinec, J. Magn. Magn. Mater. **225**(1–2), 109–112 (2001)

M. Babincova, P. Cicmanec, V. Altanerova, C. Altaner, P. Babinec, Bioelectrochemistry **55**(1–2), 17–19 (2002)

M. Babincova, D. Leszczynska, P. Sourivong, P. Babinec, J. Leszczynski, Med. Hypotheses **62**, 375–377 (2004)

Bangslabs, Bangs Laboratories, Inc. Microspheres, Online, http://www.bangslabs.com, (Page viewed on 12/Mar./2006)

A. Chanu, S. Tamaz, S. Martel, *27th Conference of IEEE–EMBs*, (IEEE, Beijing, Oct. 2006)

S.E. Charm, G.S. Kurland, *Blood Flow and Microcirculation*, (Wiley, New York, 1974)

B. Chronik, A. Alejski, B.K. Rutt, *ISMRM Conference 1999*, (ISMRM, Berkeley, CA, 1999)

V. Fidleris, R.L. Whitmore, Br. J. Appl. Phys. **12**, 490–494 (1961)

Z.G. Forbes, B.B. Yellen, K.A. Barbee, G. Friedman, IEEE Trans. Magnet. **39**(5 II), 3372–3377 (2003)

E.H. Frei, *1972 INTERMAG Conference, 10–13 April 1972: IEEE Transactions on Magnetics*, (IEEE, Los Alamitos, CA, 1972), pp. 407–413

M.S. Grady, M.A. Howard III, J.A. Molloy, R.C. Ritter, E.G. Quate, G.T. Gillies, Med. Phys. **16**, 263–272 (1989)

M.S. Grady, M.A. Howard III, W.C. Broaddus, J.A. Molloy, R.C. Ritter, E.G. Quate, G.T. Gillies, Neurosurgery **27**, 1010–1015; discussion 1015–6 (1990a)

M.S. Grady, M.A. Howard III, J.A. Molloy, R.C. Ritter, E.G. Quate, G.T. Gillies, Med. Phys. **17**, 405–415 (1990b)

A.D. Grief, G. Richardson, J. Magn. Magn. Mater. **293**(1), 455–463 (2005)

G. Guglielmi, F. Vinuela, J. Dion, G. Duckwiler, J. Neurosurg. **75**, 8–14 (1991a)

G. Guglielmi, F. Vinuela, I. Sepetka, V. Macellari, J. Neurosurg. **75**, 1–7 (1991b)

M.A. Howard, M.S. Grady, R.C. Ritter, G.T. Gillies, E.G. Quate, J.A. Molloy, Neurosurgery **24**, 444–448 (1989)

Gh. Iacob, O. Rotariu, N.J.C. Strachan, U.O. Hafeli, Biorheology **41**(5), 599–612 (2004)

R. Kehlenbeck, R. Di Felice, Chem. Eng. Technol. **21**, 303–308 (1999)

M.-C. Kim, D.-K. Kim, S.-H. Lee, M. Shahrooz Amin, I.-H. Park, C.-J. Kim, M. Zahn, IEEE Trans. Magnet. **42**(4), 979–982 (2006)

A.J. Lemke, M.I. Senfft von Pilsach, A. Lubbe, C. Bergemann, H. Riess, R. Felix, Eur. Radiol. **14**, 1949–1955 (2004)

S. Martel, J. Mathieu, L. Yahia, G. Beaudoin, G. Soulez, inventors. Method and system for propelling and controlling displacement of a microrobot in a blood vessel. US. no. 10/417, 475 (2004)

J.-B. Mathieu, S. Martel, L. Yahia, G. Soulez, G. Beaudoin, BioMed. Mater. Eng. **15**, 367–374 (2005)

J.B. Mathieu, G. Beaudoin, S. Martel, IEEE Trans. Biomed. Eng. **53**(2), 292–299 (2006)

S.R. McDougall, A.R. Anderson, M.A. Chaplain, J.A. Sherratt, Bull. Math. Biol. **64**, 673–702 (2002)

J.A. Molloy, R.C. Ritter, M.S. Grady, M.A. Howard III, E.G. Quate, G.T. Gillies, Ann. Biomed. Eng. **18**, 299–313 (1990)

M.A. Morales, T.K. Jain, V. Labhasetwar, D.L. Leslie-Pelecky, *49th Annual Conference on Magnetism and Magnetic Materials, Nov. 2004: Journal of Applied Physics*, (AIP, Melville, NY, 2005), pp. 10–905

K. Mosbach, U. Schroder, FEBS Lett. **102**, 112–116 (1979)

O. Mykhaylyk, N. Dudchenko, A. Dudchenko, J. Magn. Magn. Mater. **293**(1), 473–482 (2005)

New Era Pump systems, Syringe Pump—Advanced Precision Programmable Syringe Pumps—SyringePump.com, Online, http://www.syringepump.com/ (2006).

H. Nobuto, T. Sugita, T. Kubo, S. Shimose, Y. Yasunaga, T. Murakami, M. Ochi, Int. J. Cancer **109**, 627–635 (2004)

N. Pekas, M. Granger, M. Tondra, A. Popple, M.D. Porter, J. Magn. Magn. Mater. **293**(1), 584–588 (2005)

R.E. Rosensweig. *Ferrohydrodynamics*, (Dover, Mineola, NY, 1997)

A. Senyei, K. Widder, G. Czerlinski, J. Appl. Phys. **49**(6), 3578–3583 (1978)

Stereotaxis, Online, www.stereotaxis.com, (Page viewed on 12/Mar./2006)

D. Therriault, S.R. White, J.A. Lewis, Nat. Mater. **2**, 265–271 (2003)

Thurlby Thandar Instruments, TTi—Laboratory Power Supply Selection Table, Online, http://www.tti-test.com/products-tti/psu/psu-select.htm, (Page viewed on 30/Mar./2006)

R. Turner, J. Phys., D, Appl. Phys. **19**(8), 147–151 (1986)

R. Turner, J. Phys., E J. Sci. Instrum. **21**(10), 948–952 (1988)

R. Turner, Magn. Reson. Imaging **11**(7), 903–920 (1993)

H.J. Varghese, L.T. MacKenzie, A.C. Groom, C.G. Ellis, A.F. Chambers, I.C. MacDonald, Am. J. Physiol, Heart Circ. Physiol. **288**, H185–H193 (2005)

Varian, Cary 50 UV-Vis spectrophotometer, Online, http://www.varianinc.com/ (2006)

E. Viroonchatapan, M. Ueno, H. Sato, I. Adachi, H. Nagae, K. Tazawa, I. Horikoshi, Pharm. Res. **12**, 1176–1183 (1995)

F.M. White. *Fluid Mechanics*, 4th edn. (McGraw-Hill, New York, 1999), p. 341

R.L. Whitmore. *Rheology of the Circulation*, (Pergamon, New York, 1968)

B.B. Yellen, Z.G. Forbes, K.A. Barbee, G. Friedman, *Intermag 2003: International Magnetics Conference, Mar 28–Apr 3 2003*, (Institute of Electrical and Electronics Engineers, Los Alamitos, CA, 2003), pp. 06

B.B. Yellen, Z.G. Forbes, D.S. Halverson, G. Fridman, K.A. Barbee, M. Chorny, R. Levy, G. Friedman, J. Magn. Magn. Mater. **293**(1), 645–647 (2005)